

NANO EXPRESS

Open Access

An investigation into the conversion of In_2O_3 into InN nanowires

Polina Papageorgiou¹, Matthew Zervos^{2*} and Andreas Othonos¹

Abstract

Straight In_2O_3 nanowires (NWs) with diameters of 50 nm and lengths $\geq 2 \mu\text{m}$ have been grown on Si(001) via the wet oxidation of In at 850°C using Au as a catalyst. These exhibited clear peaks in the X-ray diffraction corresponding to the body centred cubic crystal structure of In_2O_3 while the photoluminescence (PL) spectrum at 300 K consisted of two broad peaks, centred around 400 and 550 nm. The post-growth nitridation of In_2O_3 NWs was systematically investigated by varying the nitridation temperature between 500 and 900°C, flow of NH_3 and nitridation times between 1 and 6 h. The NWs are eliminated above 600°C while long nitridation times at 500 and 600°C did not result into the efficient conversion of In_2O_3 to InN. We find that the nitridation of In_2O_3 is effective by using NH_3 and H_2 or a two-step temperature nitridation process using just NH_3 and slower ramp rates. We discuss the nitridation mechanism and its effect on the PL.

Introduction

Group III-Nitride (III-N) semiconductors have been investigated extensively over the past decades due to their applications as electronic and optoelectronic devices. In addition, they are promising for the realization of high efficiency, multi-junction solar cells since their band-gaps vary from 0.7 eV in InN through to 3.4 eV in GaN up to 6.2 eV in AlN; thereby, allowing the band gaps of the ternaries $\text{In}_x\text{Ga}_{1-x}\text{N}$ and $\text{Al}_x\text{Ga}_{1-x}\text{N}$ to be tailored in between by varying x . Nanowires solar cells (NWSCs) are also receiving increasing attention but so far they have been fabricated from Si and metal-oxide (MO) NWs. Nitride NWs such as InN [1], GaN [2] and AlN [3] are, therefore, promising for the realization of full-spectrum third generation NWSCs. However, their growth and properties must be understood beforehand in order to make nanoscale devices. So far we have grown InN [1] and GaN NWs [2] using the direct reaction of In or Ga with NH_3 , while more recently we showed that Ga_2O_3 NWs may be converted to GaN by post-growth nitridation using NH_3 and H_2 [4]. Here, we have undertaken a systematic investigation into the conversion of In_2O_3 to InN NWs, which has not been

carried out previously by others, thereby complementing our earlier work on the conversion of Ga_2O_3 to GaN NWs.

Therefore, we have grown straight In_2O_3 NWs with diameters of 50 nm and a high yield and uniformity. We find that the post-growth nitridation of In_2O_3 NWs using NH_3 leads to the elimination of the NWs above 600°C. The In_2O_3 NWs are preserved for temperatures less than 700°C but are not converted into InN even after long nitridation times of 6 h. However, the nitridation process was enhanced significantly via the use of H_2 or by employing a two-step temperature nitridation process, which also lead to a suppression of the photoluminescence (PL) peak at 550 nm similar to the nitridation of Ga_2O_3 NWs [4].

Experimental method

Initially In_2O_3 NWs were grown using an atmospheric pressure chemical vapour deposition (APCVD) reactor described elsewhere [5]. For the growth of In_2O_3 NWs, 0.2 g of fine In powder (Aldrich, Cyprus, Mesh 100, 99.99%) was weighed and loaded in a quartz boat, while square pieces of n^+ Si(001) $\approx 7 \text{ mm} \times 7 \text{ mm}$, coated with $\approx 1.0 \text{ nm}$ of Au, were loaded at various distances from the In. The Au layer was deposited via sputtering using Ar under a pressure of $\approx 10^{-2} \text{ mBar}$. The boat was positioned directly above the thermocouple used to measure the heater temperature at the centre of the 1"

* Correspondence: zervos@ucy.ac.cy

²Nanostructured Materials and Devices Laboratory, Department of Mechanical Engineering, Materials Science Group, School of Engineering, University of Cyprus, P.O. Box 20537, Nicosia, 1678, Cyprus.
Full list of author information is available at the end of the article

quartz tube (QT). Another quartz boat with ≈ 5 ml of de-ionised (DI) H_2O was positioned at the inlet of the tube. After loading the boats at room temperature (RT), Ar (99.999%) was introduced at a flow rate of 50 standard cubic centimetres per minute (sccm) for 10 min. Following this, the temperature was ramped to $850^\circ C$ under a flow of 50 sccm Ar using a ramp rate of $30^\circ C/min$. Upon reaching the growth temperature (T_G), the flow of Ar was maintained at 50 sccm for 30 min in order to grow the In_2O_3 NWs after which the reactor was allowed to cool down in a flow of 50 sccm of Ar for at least 30 min. The sample was always removed only when the temperature was lower than $100^\circ C$.

The nitridation of the In_2O_3 NWs was carried out in a new 1" QT without any solid precursors. After loading each sample with In_2O_3 NWs from the downstream side, a flow of 500 sccm Ar was introduced for 10 min after which the temperature was ramped to the nitridation temperature (T_N) under a flow of NH_3 that varied between 125 and 250 sccm using a ramp rate of $30^\circ C/min$. Upon reaching T_N , the same flow of NH_3 was maintained for various times between 1 and 6 h after which the reactor was allowed to cool down to RT under the same flow of NH_3 . A list of the different temperatures, nitridation times and NH_3 gas flows used for the nitridation of the In_2O_3 NWs are shown in Table 1. Similarly nitridation was carried out using NH_3 and H_2 . In this case, the temperature was ramped to $500^\circ C$ under a flow of NH_3 and H_2 whose relative flows varied using a ramp rate of $30^\circ C/min$. Upon reaching T_N , the same flow of NH_3 and H_2 was maintained for 1 h. The total flow of NH_3 and H_2 was kept constant at 200 sccm and a list of the different flows of H_2 is listed in Table 1. Finally, we carried out a two-step temperature process. In this case, the temperature was ramped to $500^\circ C$ under 125 sccm of NH_3 using a ramp rate of $10^\circ C/min$. Upon reaching T_N , the same flow of NH_3 was maintained for 1 h. Then, the temperature was ramped to $700^\circ C$ and the same flow of NH_3 was maintained for

30 min after which the reactor was allowed to cool down to RT.

The morphology of the as grown In_2O_3 NWs and those treated with NH_3 were examined with a TESCAN scanning electron microscope (SEM), while their crystal structure and phase purity were investigated using a SHIMADZU, X-ray diffraction (XRD-6000), with Cu-K α source, by performing a scan of $\theta - 2\theta$ in the range between 10° and 80° . Finally, PL measurements were carried using above bandgap (approx. 3.75 eV [6]) excitation at 267 nm. The pulse excitation was the second harmonic of a beam from an *optical parametric amplifier* pumped with a mode-locked TiSapphire laser. The pulses were 100 fs FWHM at a repetition rate of 250 kHz. The energy per pulse incident on the samples was 40 pJ over a spot of 2 mm in diameter.

Results and discussion

Previously, we obtained In_2O_3 NWs by dry oxidation at $700^\circ C$ [7]. A high yield of In_2O_3 NWs with an average diameter of ≈ 100 nm and lengths of $\approx 1 \mu m$ was obtained on Si(111) and quartz. However, these In_2O_3 NWs were slightly tapered; their diameters were larger and lengths were shorter compared to the In_2O_3 NWs obtained here by wet oxidation. Moreover, the distribution of the In_2O_3 NWs obtained by wet oxidation was far superior and much more uniform compared to those obtained by dry oxidation. A typical image of In_2O_3 NWs that were obtained at $T_G = 850^\circ C$ by wet oxidation is shown in Figure 1. It should be pointed out that a high yield and uniform distribution of In_2O_3 NWs extending over $1 cm^2$ was obtained when the distance between the In and the Au/n $^+$ Si (001) was ≥ 15 mm, which led to a light blue-like deposit. The In_2O_3 NWs

Table 1 Summary of post-growth nitridation conditions for the conversion of In_2O_3 NWs to InN

(I) T_N ($^\circ C$)	(II) t (h)	(III) % H_2
CVD797	500 $^\circ C$	CVD850 500 $^\circ C$, 3 h
CVD788	600 $^\circ C$	CVD853 500 $^\circ C$, 6 h
CVD790	800 $^\circ C$	CVD795 600 $^\circ C$, 1 h
CVD791	900 $^\circ C$	CVD849 600 $^\circ C$, 2 h
		CVD859 80
		CVD848 600 $^\circ C$, 3 h

Initially a flow of 500 sccm of Ar was introduced into the reactor after which the temperature was ramped to T_N at $30^\circ C/min$ under a flow of (I) 250 sccm of NH_3 , (II) 125 sccms of NH_3 and (III) under different flows of NH_3 and H_2 , but keeping the total flow constant at 200 sccm. Upon reaching T_N , the same flows were maintained for 1 h at various temperatures (I), different nitridation times at 500 and $600^\circ C$ (II) and for 1 h at $500^\circ C$ (III).

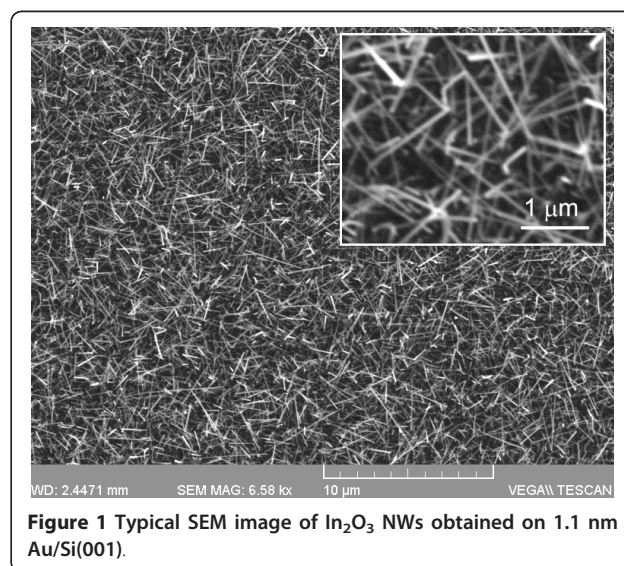


Figure 1 Typical SEM image of In_2O_3 NWs obtained on 1.1 nm Au/Si(001).

have diameters of ≈ 50 nm, lengths ≥ 2 μm and exhibited clear peaks in the XRD as shown in Figure 2 by the top curve, corresponding to the body centred cubic (bcc) crystal structure of In_2O_3 with $a = 10.12$ Å, in agreement with Dai et al. who obtained twisted In_2O_3 NWs by wet oxidation [8]. The In_2O_3 NWs shown in Figure 1 are straight [9,10] and in our case In_2O_3 NWs grow by a simple chemical route involving the following reaction: $2\text{In} + 3\text{H}_2\text{O} \rightarrow \text{In}_2\text{O}_3 + 3\text{H}_2$ [8]. Wet oxidation is a facile method and generally occurs faster than dry oxidation. No NWs were obtained on plain Si(001), suggesting the growth of In_2O_3 NWs occurs via the vapour-liquid-solid (VLS) mechanism with Au acting as the catalyst. In this case, Au NPs absorb In until they become supersaturated after which In_2O_3 NW growth commences via the reaction of In with H_2O as outlined above.

The PL spectrum following excitation at 267 nm at 300 K consisted of two broad peaks, centred at 400 and 550 nm as shown in Figure 3. Similar peaks in the PL have been observed by Yan et al. [11] who obtained a broad luminescence band centred at 395 nm from In_2O_3 nanorods, Liang et al. [12] who found a peak at 470 nm from In_2O_3 nanofibres and Wu et al. [13] who observed two distinct peaks at 416 and 435 nm from In_2O_3 nanowires. It is important to point out that these peaks are commonly attributed to the presence of oxygen vacancies.

Next, we will describe the conversion of In_2O_3 NWs into InN and in particular consider the nitridation of In_2O_3 NWs at different temperatures. To begin with In_2O_3 NWs were subjected to 250 sccm of NH_3 for 1 h

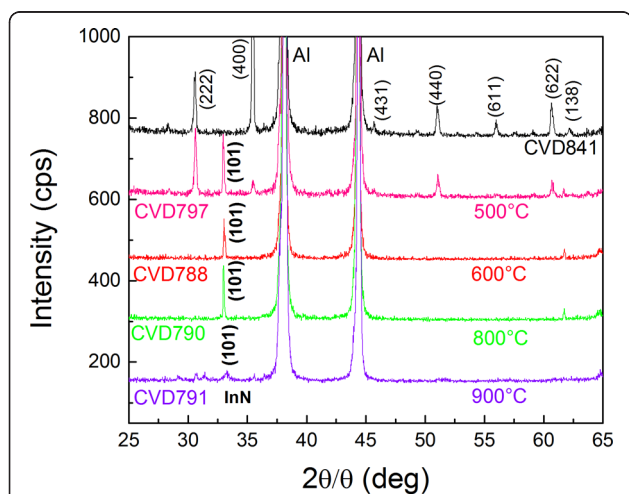


Figure 2 XRD of In_2O_3 NWs obtained after nitridation at different temperature as listed in Table 1. Note that CVD841 shown at the top corresponds to the as grown In_2O_3 NWs. The InN related peaks are shown in bold, while the Al peaks belong to the holder and have also been identified.

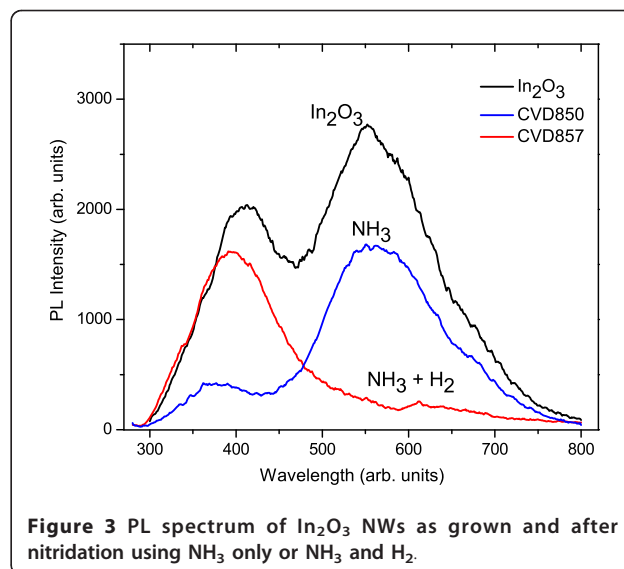
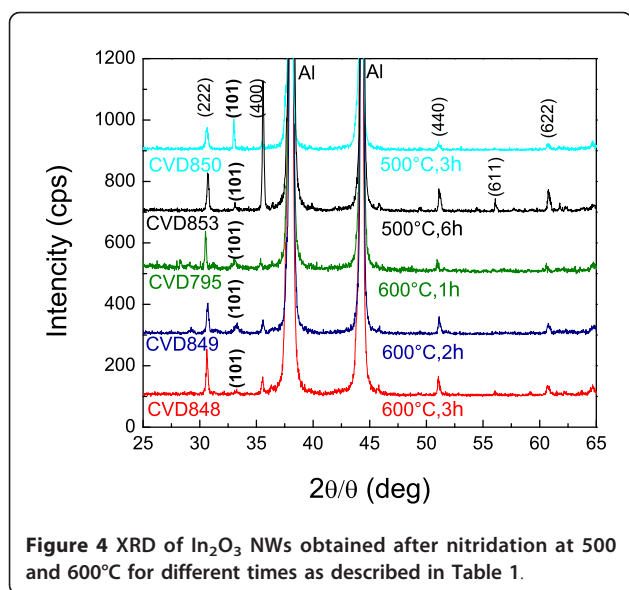


Figure 3 PL spectrum of In_2O_3 NWs as grown and after nitridation using NH_3 only or NH_3 and H_2 .

at various temperatures between 500 and 900°C as listed in Table 1.

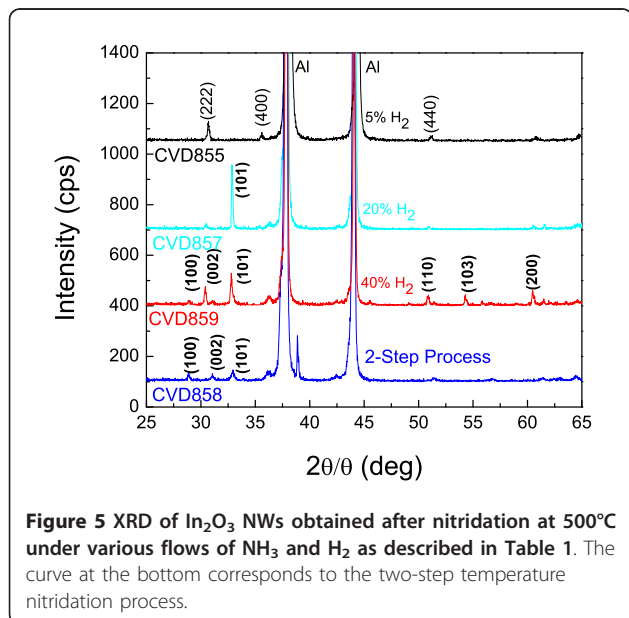
The XRD spectra of the In_2O_3 NWs treated at different temperatures is shown in Figure 2. As can be seen most of the oxide peaks disappear at temperatures $>600^\circ\text{C}$. However, a new peak appears, which corresponds to the (101) crystallographic direction of InN [1]. Furthermore, SEM images reveal that the In_2O_3 NWs have been eliminated above 600°C, but a thin layer of InN remains on the Si(001). Evidently, the nitridation of the In_2O_3 NWs is destructive above 600°C due to the fast decomposition of In_2O_3 to In_2O , which is a gas. We should also point out that in addition to the temperature we also varied the nitridation time. In particular, we carried out nitridations of In_2O_3 NWs at 500 and 600°C under a flow of 125 sccm NH_3 for different times as described in Table 1.

Again the conversion of In_2O_3 NWs to InN appears to be incomplete as can be clearly seen from the XRD spectra in Figure 4 where one can observe the presence of In_2O_3 peaks and just one peak at (101) corresponding to InN. In order to achieve the efficient conversion of In_2O_3 NWs to InN without eliminating them, we used two different approaches. In the first one, we have carried out post-growth nitridation, which included H_2 as shown in Table 1 and in the second approach, we have utilised a two-step temperature nitridation process. The corresponding XRD spectra are shown in Figure 5. As can be seen from the XRD spectra, H_2 plays a significant role in the removal of the oxygen and thus all major oxide peaks are eliminated and the conversion to InN is achieved with 40% H_2 . As already described above, NH_3 alone does not promote the efficient conversion of In_2O_3 NWs into InN at temperatures between 500 and



600°C. This is likely due to the formation of an InN shell around the In_2O_3 , which prevents the diffusion of N into the In_2O_3 core. However, H_2 appears to promote the conversion of In_2O_3 into InN [14].

In addition, the two-step process lead to the effective conversion of In_2O_3 NWs to InN using just NH_3 . In this case, the temperature was ramped at 10°C/min up to 500°C and held constant over a period of 1 h, after which the temperature was ramped again slowly to 700°C in order to promote the nitridation. Recall that the In_2O_3 NWs were eliminated during a single-step nitridation process at 700°C using a fast ramp rate of 30°C/min. However, it should be noted that the NWs



treated by this two-step temperature nitridation process were bent probably due to the fact that the crystal structure changes from bcc to the hexagonal wurtzite structure, and there is a non-uniform strain distribution between the core and shell. The effect of the post-growth nitridations on the PL of the In_2O_3 NWs is shown in Figure 3.

In the case of the nitridation using just NH_3 for 3 h at 500°C, one may observe that there is no substantial change in the shape of the PL of the In_2O_3 NWs except from the fact that the PL intensity has been reduced. However, the nitridation of the In_2O_3 NWs using NH_3 and H_2 leads to a clear suppression of the peak at 550 nm, which is attributed to oxygen consistent with previous investigations on Ga_2O_3 [4]. The peak around 400 nm maybe attributed to In vacancies [15], but not O_2 as commonly suggested [11-13]. However, further work is required to clarify the origin of the PL peak around 400 nm.

Conclusions

Straight In_2O_3 NWs with diameters of 50 nm, lengths $\geq 2 \mu\text{m}$ and a bcc crystal structure have been grown on Au/Si(001) via the wet oxidation of In at 850°C. These exhibited two broad peaks in the PL, centred around 400 and 550 nm. The post-growth nitridation of In_2O_3 NWs was found to be effective by using NH_3 and H_2 at 500 and 600°C or a two-step temperature, nitridation process at 500 and 700°C. This lead to a suppression of the PL peak around 550 nm related to O_2 consistent with previous investigations on Ga_2O_3 . In contrast, single-step temperature, nitridations using just NH_3 , carried out with fast ramp rates above 600°C lead to the complete elimination of the In_2O_3 NWs, while they were not effective at 500 and 600°C.

Abbreviations

APCVD: atmospheric pressure chemical vapour deposition; bcc: body centred cubic; DI: de-ionised; MO: metal-oxide; NWs: nanowires; NWSCs: nanowires solar cells; PL: photoluminescence; QT: quartz tube; RT: room temperature; SEM: scanning electron microscope; VLS: vapour-liquid-solid; XRD: X-ray diffraction.

Acknowledgements

This work was supported by the Research Promotion Foundation of Cyprus under grant BE0308/03.

Author details

¹Department of Physics, Research Centre of Ultrafast Science, University of Cyprus, P.O. Box 20537, Nicosia, 1678, Cyprus. ²Nanostructured Materials and Devices Laboratory, Department of Mechanical Engineering, Materials Science Group, School of Engineering, University of Cyprus, P.O. Box 20537, Nicosia, 1678, Cyprus.

Authors' contributions section

MZ and PP carried out the growth, scanning electron microscopy and x-ray diffraction measurements. AO carried optical characterization. All authors read and approved the final manuscript.

Competing interests

The authors declare that they have no competing interests.

Received: 9 December 2010 Accepted: 7 April 2011

Published: 7 April 2011

References

1. Othonos A, Zervos M, Pervolaraki M: **Ultrafast Carrier Relaxation in InN Nanowires Grown by Reactive Vapor Transport.** *Nanoscale Res Lett* 2009, **4**:122.
2. Tsokkou D, Othonos A, Zervos M: **Defect states of chemical vapor deposition grown GaN nanowires: Effects and mechanisms in the relaxation of carriers.** *J Appl Phys* 2009, **106**:05431.
3. Li J, Nam KB, Nakarmi ML, Lin JY, Jiang HX, Pierre Carrier, Su-Huai Wei: **Band structure and fundamental optical transitions in wurtzite AlN.** *Appl Phys Lett* 2003, **83**:5163.
4. Othonos A, Zervos M, Christofides C: **A systematic investigation into the conversion of β -Ga₂O₃ to GaN nanowires using NH₃ and H₂: Effects on the photoluminescence properties.** *J Appl Phys* 2010, **108**:124319.
5. Zervos M, Othonos A: **Synthesis of Tin Nitride SnxNy Nanowires by Chemical Vapour Deposition.** *Nanoscale Res Lett* 2009, **4**:1103.
6. Aron Walsh, Da Silva Juarez LF, Su-Huai Wei, Körber C, Klein A, Piper LFJ, Alex DeMasi, Smith Kevin E, Panaccione G, Torelli P, Payne DJ, Bourlange A, Egdel RG: **Nature of the Band Gap of In₂O₃ Revealed by First-Principles Calculations and X-Ray Spectroscopy.** *Phys Rev Lett* 2008, **100**:167402.
7. Tsokkou D, Othonos A, Zervos M: **Ultrafast time-resolved spectroscopy of In₂O₃ nanowires.** *J Appl Phys* 2009, **106**:084307.
8. Dai L, Chen XL, Jian JK, He M, Zhou T, Hu BQ: **Fabrication and characterization of In₂O₃ Nanowires.** *Appl Phys A* 2002, **75**:687.
9. Qurashi A, El-Maghraby EM, Yamazaki T, Kikuta T: **Catalyst supported growth of In₂O₃ nanostructures and their hydrogen gas sensing properties.** *Sensors and Actuators B* 2010, **147**:48.
10. Calestani D, Zha M, Zappettini A, Lazzarini L, Zanotti L: **In-catalyzed growth of high-purity indium oxide nanowires.** *Chem Phys Lett* 2007, **445**:251.
11. Yan Y, Zhou L: **Competitive growth of In₂O₃ nanorods with rectangular cross sections.** *Appl Phys A* 2008, **92**:401.
12. Liang C, Meng G, Lei Y, Phillipp F, Zhang L: **Catalytic Growth of Semiconducting In₂O₃ Nanofibers.** *Adv Mater* 2001, **13**:1330.
13. Wu XC, Hong JM, Han ZJ, Tao YR: **Fabrication and photoluminescence characteristics of single crystalline In₂O₃ nanowires.** *Chem Phys Lett* 2003, **373**:28.
14. Gao L, Zhang Q, Li J: **Preparation of ultrafine InN powder by the nitridation of In₂O₃ or In(OH)₃ and its thermal stability.** *J Mater Chem* 2003, **13**:154.
15. Zhang J, Xu B, Jiang F, Yang Y, Li J: **Fabrication of ordered InN nanowire arrays and their photoluminescence properties.** *Phys Lett A* 2005, **337**:121.

doi:10.1186/1556-276X-6-311

Cite this article as: Papageorgiou et al.: An investigation into the conversion of In₂O₃ into InN nanowires. *Nanoscale Research Letters* 2011 **6**:311.

Submit your manuscript to a SpringerOpen® journal and benefit from:

- Convenient online submission
- Rigorous peer review
- Immediate publication on acceptance
- Open access: articles freely available online
- High visibility within the field
- Retaining the copyright to your article

Submit your next manuscript at ► springeropen.com